IEEE Access
Multidisciplinary | Rapid Review | Open Access Journal

Received July 10, 2019, accepted July 29, 2019, date of publication August 7, 2019, date of current version August 21, 2019.

Digital Object Identifier 10.1109/ACCESS.2019.2933689

A Novel Fractional Frequency Reuse Scheme for Interference Management in LTE-A HetNets

SAJJAD AHMAD KHAN[1], ADNAN KAVAK[1], SULTAN ALDIRMAZ ÇOLAK[2], AND KEREM KÜÇÜK[1]

[1]Department of Computer Engineering, Kocaeli University, 41950 Kocaeli, Turkey
[2]Department of Electronics and Communication Engineering, Kocaeli University, 41950 Kocaeli, Turkey

Corresponding author: Adnan Kavak (akavak@kocaeli.edu.tr)

This work was supported by the Kocaeli University Scientific Research Unit under Grant 2017/061.

ABSTRACT The Heterogeneous Network (HetNet) has emerged as one of the most promising developments toward achieving the target of the Long Term Evolution-Advanced (LTE-A) systems. However, Co-Channel Interference (CCI) is one of the critical challenges of HetNet, that degrades the overall performance of a system. Therefore, an appropriate Radio Resource Management (RRM) mechanism is required to deploy and expand the HetNets properly. In this paper, a new RRM strategy called Fractional Frequency Reuse with Three Sectors and Three Layers (FFR-3SL) technique is proposed. The FFR-3SL efficiently utilizes the radio resources and alleviates the effects of CCI in LTE-A HetNets and thereby improving the system performance. In order to implement the proposed strategy, the entire macrocell coverage area is segmented into three sectors and three layers, while the total bandwidth is divided into seven subbands. Subsequently, the subbands are accurately distributed among femtocells and macrocells by employing the proposed algorithm. As a result, the co-tier and cross-tier interferences are managed on a prior basis. The Monte Carlo simulation is performed to evaluate and compare the performance of the proposed method with the existing methods. The simulation results show that the proposed method achieves higher throughput and better capacity in LTE-A HetNet system. Furthermore, the efficiency of the system is improved with regard to user satisfaction in terms of signal to interference and noise ratio (SINR) values.

INDEX TERMS Co-Channel interference (CCI), femtocell, fractional frequency reuse (FFR), heterogeneous network (HetNet), long term evolution-advanced (LTE-A), radio resource management (RRM).

NOMENCLATURE

PL	Path Loss.
M	Macrocell.
F	Femtocell.
ω	Total number of RBs.
K	Total number of subbands.
S	Total number of cell sectors.
L	Total number of cell layers.
SB	Set of subbands.
Ω	Set of subbands in each sector.
$G^k_{m,M}$	Channel gain between macrocell M and MUE m at subcarrier k.
$G^k_{f,F}$	Channel gain between femtocell F and FUE f at subcarrier k.
$SINR^k_m$	SINR value received by MUE m at subcarrier k.
$SINR^k_f$	SINR value received by FUE f at subcarrier k.
P^k_M	Transmit power of macrocell M at subcarrier k.
P^k_F	Transmit power of femtocell F at subcarrier k.
N_o	White noise power density.
Δf	Center frequency.
P_{tx}	Macrocell transmit power for each layer.
C^k_m	Capacity achieved by MUE m at subcarrier k.
C^k_f	Capacity achieved by FUE f at subcarrier k.
Υ_{rx}	Min. detectable RSRP (dB) at the edge of each layer.
φ^M_i	Set of frequencies received at femtocell (F_i) from macrocells (M).
φ^F_i	Set of frequencies received at femtocell (F_i) from other femtocells.
T_X	Throughput achieved by femtocell F or macrocell M.

The associate editor coordinating the review of this manuscript and approving it for publication was Florin Pop.

This work is licensed under a Creative Commons Attribution 4.0 License. For more information, see http://creativecommons.org/licenses/by/4.0/

T_{total}	The overall throughput achieved whether by macrocells M or by femtocells F.
λ	Group of usable SBs for femtocell (F_i) in a sector.
$\setminus$	Indicates exclusion in set theory.
$\zeta_{i,j}^{F}$	Group of frequencies received from femtocells of other sectors.
ψ_{x}^{k}	Notifies the assignment of subcarrier k to UEs x.
$\varphi_{i,j}^{F}$	Group of frequencies received from other femtocells of the same sector.
$\varphi_{i}^{assigned}$	The assigned frequency SB to the femtocell (F_i).
η	Efficiency achieved by the system.
ρ	Ratio of user distribution in the central layer.
Γ_{thr}	SINR threshold.
q	Ratio of central layer radius to cell radius.
N_{UE}	Total Number of UEs in a cell.
$N_{UE,c}$	Number of UEs in the central layer.

I. INTRODUCTION

The telecommunication industry progresses toward the development of the Fifth Generation (5G) standard that requires coexistence of Heterogeneous Networks (HetNets). The reason for using HetNets is to provide effective wireless coverage to mobile subscribers and other wireless appliances in both indoor and outdoor environments. In other words, the demand for wireless services at indoor environment continuously increases as the mobile subscribers grow [1]. It is foreseen that by the end of 2021, two-thirds of mobile subscribers will consume data in the indoor environment [2], [3]. Therefore, HetNet appears as an adequate solution for the envisioned 5G mobile cellular networking system. In specifications of the Long Term Evolution-Advanced (LTE-A) networks, a HetNet is a multi-tier network system, where different small-cells are deployed especially in crowded areas and cell-edges over the existing cellular networks [4]. Small-cells are short ranged, low powered, and easy to plug-in radio access nodes using licensed and unlicensed frequency bands [5]. The small-cells consist of relay nodes, microcells, picocells, and femtocells, which are deployed at different places according to user requirements. One of the significant types of small-cells is femtocell, which can be located at homes, offices, and public places to provide coverage to the indoor subscribers. According to the Third Generation Partnership Project (3GPP) Release-12, a femtocell is also known as Home evolved Node Base-Station (HeNB) [6]. It covers relatively smaller areas, i.e., 20 to 30 meters and provides high data throughput to the User Equipment (UE). Thanks to femtocells, users who are in the edges and shadow areas of a macrocell region can also be served. Furthermore, 5G Internet of Things (IoT) systems may also employ femtocells in order to connect home appliances to the core network of the system [7].

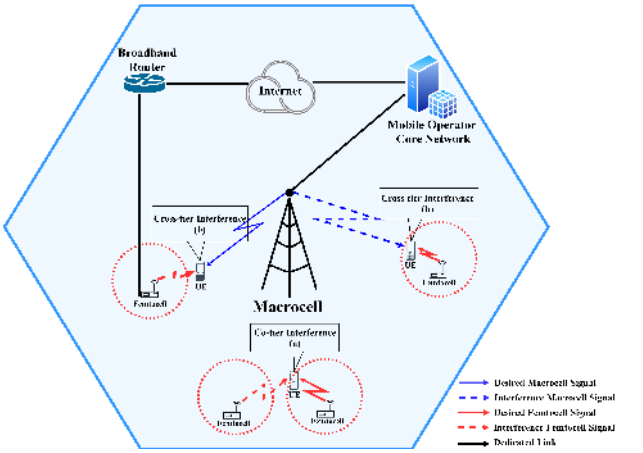

FIGURE 1. The CCI scenarios for down-link case.

In LTE-A HetNet system, macrocells and femtocells are operating on the same frequency channel. As a result, Co-Channel Interference (CCI) occurs. There are two major types of CCI, described in Fig. 1, which may arise in different situations. When the CCI occurs among the same type of cells i.e., femtocell-femtocell, it is called co-tier interference, like scenario **(a)** depicted in Fig. 1. While on the other hand, the CCI among different type of cells is called cross-tier interference, as shown in scenario **(b)** of Fig. 1. Ultimately, interference degrades the quality of the signal and creates critical problems during wireless communication. Therefore, different methods are suggested in the literature to control CCI in HetNets. Dedicated channel link is the most straightforward technique to solve this issue; however, there is a high probability of wasting the radio resources [8]. Moreover, Carrier Aggregation (CA) and Enhanced Inter-Cell Interference Coordination (E-ICIC) methods are introduced in 3GPP Release-12 [9]. Besides that, researchers are still investigating different techniques and comparing them to find out the best solution. In [10], a Power Control Algorithm (PCA) and simulation tool are introduced to reduce the co-tier interference among femtocells. In [11], L. Zhang *et al.* suggest a cognitive radio approach, where the neighboring femtocells exchange the path-loss information to each other and select the carriers aggregation to estimate the co-tier interference. The above two approaches consider only co-tier interference but ignore the cross-tier interference completely.

Fractional Frequency Reuse (FFR) as a resource allocation scheme is an effective technique used to reduce the CCI in LTE-A HetNets [12], [13]. The authors in [14] investigated the FFR and non-FFR approaches and expressed that the FFR scheme performs much better than non-FFR in terms of throughput and capacity. Consequently, many researchers studied different FFR schemes [15]–[21]. The authors in [22], present an Optimal Static FFR (OSFFR) scheme for two-tier HetNets in LTE-Advanced systems in order to increase throughput in macrocell edge UEs and they compare four different FFR schemes, i.e., strict FFR, soft FFR, FFR-3, and OSFFR schemes. According to their simulation results,

TABLE 1. Summary of existing popular FFR schemes and proposed FFR scheme used in two-tiered HetNets.

Technique	Layers	Sectors	Zones	SBs	Merits	Demerits
OSFFR [22]	2	6	12	7	Mitigate cross-tier interference and improve the throughput of edge femtocells	Hard to implement and chances of co-tier interference among femtocells.
FFR-3R [23]	3	3	9	4	Achieve better throughput than no-FFR and FFR-2 techniques.	Inter-subband interference may occur.
FFR-3 [24]	2	3	6	4	Alleviate cross-tier interference and perform better than no-FFR scheme.	Co-tier interference may occur among femtocells.
FFR-3SL (Proposed)	3	3	9	7	Consider both cross-tier and co-tier interferences. Improved data throughput as compared to existing methods.	Assumption that majority of users demanding high bandwidth are located at the central layers.

OSFFR scheme outperforms the other three state-of-the-art FFR schemes. Nevertheless, the subband distribution among femtocells is not addressed, therefore, co-tier interference may occur among femtocells. N. Fradi *et al.* in [23], proposed a resource allocation scheme using FFR with three regions (FFR-3R) in LTE-A Orthogonal Frequency Division Multiple Access (OFDMA) based HetNet. The simulation results show an improvement in macrocells throughput because of the decline in cross-tier interference, however, the effect of co-tier interference remains the same. A similar study is presented in [24], [25], where the authors employ the same FFR scheme with three sectors (FFR-3) to overcome the effect of CCI in HetNet. The cross-tier interference is reduced and edge layer UEs achieve higher throughput. The co-tier interference among femtocells is not addressed properly.

In this paper, a new FFR strategy is proposed for LTE-A HetNets, where the whole macrocell coverage area is segmented into three sectors and three layers. While on the other hand, the total radio frequency band is divided into seven frequency subbands (radio resources). The bigger chunk of the frequency band is shared among the entire central layer while the other subbands are distributed over the remaining zones of the middle and outer-most layers. Furthermore, the subbands are re-used by femtocells in other zones of the macrocell coverage area in a specific and well-organized manner. In order to implement our strategy, a novel FFR algorithm is proposed, which reduces not only CCI but also tries to find the most suitable subband for newly deployed femtocell when it switches on in any sector or zones of the macrocell region. A Monte Carlo simulation is performed to accurately assess the performance of our proposed method. Unlike the existing studies in literature, we focus on the central area because we assume that the central area is highly populated zones. The major contribution of this paper is to propose a new FFR scheme such that it provides reduced co-tier and cross-tier interferences, improved Femto UEs (FUEs) and Macro UEs (MUEs) throughput, better efficiency of the active UEs connection, and UE satisfaction for higher radio resources demand.

The variables (symbols), which are used in this paper are summarized in nomenclature. The remainder of this paper is organized as follows. Existing FFR methods are explained in Section-II. The system model is given in Section-III. Section-IV presents the proposed FFR-3SL algorithm, while performance evaluation metrics are given and explained in Section-V. In Section-VI, simulation model and results are discussed. The conclusion is given in Section-VII.

II. EXISTING FFR METHODS

The most favorable and reliable technique to manage and control CCI in HetNets is FFR scheme, where the radio resources (subbands) are properly allocated among femtocells and macrocells. The basic idea behind the FFR technique is to divide the total bandwidth into several small subbands and then assign to different zones of the macrocell region. Furthermore, the same subbands are re-used by femtocells in other zones of the macrocells region, separated by considerable distance to avoid interference. However, the macrocell coverage area must be segmented in an organized manner, in order to reduce the effect of CCI. In this paper, three most cited methods are considered and summarized in Table 1.

A. OSFFR

The OSFFR scheme is proposed by N. Saqueb *et al.* in [22], where the macrocell coverage area is split into two layers and six sectors. As a result, the macrocell is segmented into twelve total zones, on the other hand, the total available bandwidth is divided into seven subbands. The first (SB) is shared among all the zones of the central layer, while the remaining subbands are distributed among the six zones of edge layer of the macrocell region. In addition, all the subbands are re-used by femtocells in different zones of the macrocell coverage

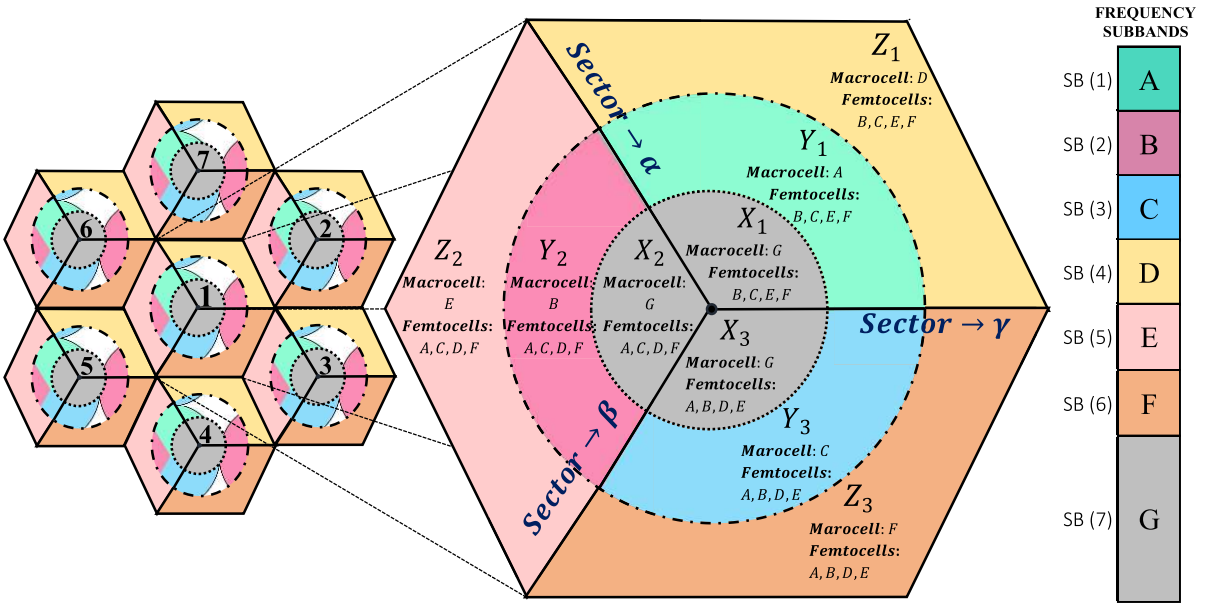

FIGURE 2. A HetNet topology of the proposed FFR-3SL method.

area in such a way to avoid the cross-tier interference. This scheme improves the performance of the system and reduces cross-tier interference, nevertheless, co-tier interference is not rectified properly. Moreover, the effect of Macro Base Station (MBS) transmit power among narrow sectors is quite difficult to manage in this scheme.

B. FFR-3R

Another FFR strategy with three regions (FFR-3R) is presented in [23] by Fradi *et al.*, where the entire macrocell coverage area is separated into three layers, named as inner, intermediate and outer regions. Alongside, the macrocell coverage area is further split into three sectors. In order to fulfill the nine zones, the total available bandwidth is divided into four (A, B, C, D) subbands. The subband A is shared among all the center zones, while other subbands (B, C, D) are shared among different zones of intermediate and outer regions. Furthermore, all the subbands are re-used by femtocells in different zones of the macrocell coverage areas. In this scheme, the allotment of subbands is not configured efficiently. As a result, higher chances of CCI may occur among MUEs and FUEs due to frequency re-use factor.

C. FFR-3

P. Lee *et al.* suggested an idea in [24] by using the FFR method along with three sectors (FFR-3) and two layers. In this method, the overall macrocell coverage area is separated into central and edge layers. Likewise, each layer is then split into three sectors. As a result, the macrocell is segmented into six total zones. Contrarily, the total available bandwidth is divided into four subbands. The first subband is thoroughly shared among all the zones of the central layer, while the other three subbands are distributed among edge layer's zones of the macrocell region. Additionally, all the subbands are re-used by femtocells in other zones of the macrocell region. This strategy is very useful to avoid cross-tier interference, however, there is no proper mechanism explained to mitigate the co-tier interferences when it happens.

III. SYSTEM MODEL

Our new method referred to as Fractional Frequency Re-use with Three Sectors, and Three Layer (FFR-3SL) is presented in this paper. The principle idea of the proposed method is to divide the total allocated frequency band into smaller fractions (subbands), which are then distributed among femtocells and macrocell in different areas of the macrocell coverage area to assign users. The detailed network topology and a viable algorithm of the proposed method are discussed below.

The proposed network topology is demonstrated in Fig. 2, where the total frequency band is divided into seven subbands such as A, B, C, D, E, F and G. Furthermore, the whole macrocell coverage area is partitioned into three sectors, named as sector α, sector β, and sector γ, which are further segmented into three layers, named as central layer X, middle layer Y, and outer layer Z. For simplicity, we call the central layer as X_1, X_2, and X_3, middle layer as Y_1, Y_2, and Y_3 and the outermost layer as Z_1, Z_2, and Z_3 zones. According to the proposed model, the subband G is solely reserved for MUEs available in the central layer. However, the subband G is not assigned to femtocells to re-use for FUEs in the other zones of the macrocell coverage region, because it is assumed that the number of MUEs is largely available in the central layer and quite close to MBS, and they should be given priority to

use dedicated subband G. On the other hand, the subbands A, B, C, D, E, and F are reserved for MUEs in zones Y_i and Z_i ($i \in \{1, 2, 3\}$), respectively. After setting the subbands assignment for MUEs in macrocell regions, all the subbands except subband G are re-used by femtocells located in the other zones of the macrocell coverage area. Considering subband allocation among femtocells appropriately, groups of available subbands are defined for every sector. When a new femtocell is switched on, the system identifies its location by checking the reference signal received power (RSRP) values received from MBS, where RSRP is the predefined frequency measurement affix in reference signal [26]. Once, it identifies its location, then the most suitable subband is assigned to the i^{th} femtocell from the relevant group of subbands. An OFDMA based LTE-A HetNet system is used to investigate and compare the proposed method with the current methods. In the LTE-A network system, the smallest unit to be allocated to every UE in the frequency domain of the downlink channel is the resource block (RB), where each RB consists of 12 subcarriers. In term of the femtocell, an open access policy is adopted to utilize all the resources efficiently.

In the proposed model, a downlink wireless propagation channel model is considered, which comprises of path-loss (PL), log-normal shadowing and small-scale fading between Base Station (BS) and UE. The UEs are randomly distributed with a uniform distribution over the macrocell coverage area. Besides, a single wall penetration loss is used from indoor to outdoor transmission and vice-versa, while double wall penetration loss is used among indoor to indoor transmissions.

The indoor PL model is defined in 3GPP Release-13 for LTE-A HetNet system [27] as given by,

$$PL(dB) = 38.5 + 30log_{10}(d) + n \tag{1}$$

where, term d is the distance between transmitter and receiver (in meters), while n is the wall penetration loss factor, if the distance is less than or equal to 10 meters, the n is 7 dB, if the distance is greater than 10 meters and less than or equal to 20 meters, the n is 10 dB. However, if the distance greater than 30 meters, then the n is 15 dB.

Assuming a Rayleigh fading channel, the channel gain is defined as [28],

$$G = 10^{(-PL+X_\sigma)/10}|h|^2 \tag{2}$$

where PL denotes path-loss in dB and X_σ is the shadowing effect of normal (Gaussian) distribution. h is a circularly symmetric complex Gaussian random variable with zero-mean and unit variance. So, $|h|$ is Rayleigh distributed.

IV. THE PROPOSED ALGORITHM: FFR-3SL

In order to implement our new RRM strategy, we proposed a new algorithm so called FFR-3SL, which is given in Algorithm 1. The algorithm performs two primary functions. Firstly, it finds the total number of subbands and allocates them to appropriate zones in the macrocell coverage area. Secondly, it involves in selecting the most suitable subband for the femtocell deployed inside the coverage area of a macrocell. The second function avoids the chances of co-tier interference before it happens. The algorithm initially requires predefined parameters, where it takes total available RBs (ω), the total number of subbands (K), number of sectors per cell (S) and number of layers per cell (L). The number of RBs which are to be assigned for MUEs in the central zones is calculated as [22],

$$SB(K) = \omega\left(\frac{r_c}{R}\right) \quad , \tag{3}$$

and the remaining RBs for MUEs and FUEs in the middle and outer layers are calculated as,

$$SB(n) = \frac{[\omega - SB(K)]}{K-1}, \quad n = 1, 2, 3, ..., K-1 \tag{4}$$

where ω is total available RBs, r_c is the macrocell central layer radius and R is the macrocell radius as depicted in Fig. 3. K is the total number of subbands.

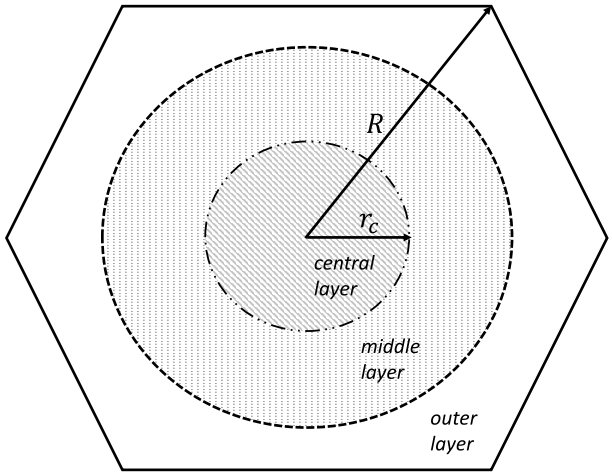

FIGURE 3. A ratio between central layer radius (r_c) and macrocell outer layer radius (R).

Example: In LTE-A network, each RB consists of 12 subcarriers and each subcarrier occupies 15 KHz. In other words, one RB occupies $12 \times 15 = 180$ KHz. Assume, if the system has 20 MHz bandwidth, 2 MHz is used for guard-band, while 18 MHz bandwidth is used for communication. The total number of RBs is, 18 MHz/180 KHz = 100 RBs.

Now, as stated in the network topology in Fig. 2, we divide the total available bandwidth into seven subbands, and if the ratio of center radius to radius of macrocell $r_c/R = 0.4$, then the total number of RBs for seventh subband G used in the central layer zones is obtained by using (3), $SB(7)$ is equal to 40 RBs.

In the same way, we can obtain the number of RBs for the remaining six subbands (A, B, C, D, E, F) which are utilized in middle and outer layers' zones of the macrocell coverage area by using (4); as a result, $SB(1 \text{ to } 6)$ equals to 10 RBs per each SB. According to the above assumptions, all the SBs

Algorithm 1 Radio Resources (Subbands) Allocation Algorithm

// Subbands Assignment to Macrocell Regions
// *Initialization*
$\omega \leftarrow RBs$; // total available resource blocks (RBs)
$K \leftarrow Subbands$; // total number of subbands
$S \leftarrow Sectors$; // total number of sectors, $S < K$
$L \leftarrow Layers$; // total number of layers, $L < K$
$SB(K) \leftarrow$ Equation 3; // central subband
$SB(n) \leftarrow$ Equation 4; // rest of the subbands
// *Allotment of subbands to each layer's zone and group them in sectors*
for $n = 1 : S$ **do**
    $X_n = SB(K)$; // subbands for central layer
    $Y_n = SB(n)$; // subbands for middle layer
    $Z_n = SB(n+S)$; // subbands for outer layer
    $\Omega_n = [SB(n), SB(n+S), SB(K)]$; // group of subbands for each sector e.g., $[\alpha, \beta, \gamma]$
end
// *Obtain the length of radius for central, middle, and outer layers*
$P_{tx} \leftarrow Input$; // set-up max. transmit power (dB) for central, middle and outer layers
$\Upsilon_{rx} \leftarrow Input$; // set-up min. detectable RSRP (dB) received at the edge of each layer (Receiver Sensitivity)
$d(m) = PLcalculation(P_{tx}, \Upsilon_{rx})$; // calculate the max radius for each layer by using the path-loss function
// Finding the best available subband for every femtocell (F)
for $i = 1$*: All femtocells* (N_{Fc}) **do**
    $F_i \leftarrow Initialize$;
    φ_i^M; // store the max. RSRP received at i^{th} femtocell (F_i) from macrocells (M) except the RSRP received from SB(K), (we assume that cell IDs are inserted in the transmitted signal of macrocells)
    if $\varphi_i^M \in \Omega_n$ **then**
        $\lambda_i = SB \setminus \Omega_n$; // subtract group of SBs used by macrocell (M) in that sector and get a group of available SBs for F_i
    end
    // *Checking for nearby femtocells*
    for $j = 1$*: All the femtocells* (N_{Fc}^s) *in sector 's' if* $(j \neq i)$ **do**
        if $j \leq K - S$ **then**
            $\varphi_i^{assigned} = \lambda_i(j)$;
        else
            $\zeta_{i,j}^F$; // store the RSRP values received at F_i from femtocells of other sectors
            $\varphi_{i,j}^F$; // store all the received RSRP values at F_i from nearby femtocells of the same sector
            if $\varphi_{i,j}^F \in \lambda_i$ **then**
                $l = arg[max(PL(d_{i,j}^F))]$
                $\varphi_i^{assigned} = \varphi_{i,j,l}^F$;
            end
        end
    end
end

are allocated to the respective zones in each layer. Once all the SBs are distributed among macrocell regions, the SBs are grouped according to their relevant sectors.

The second step of the proposed algorithm is essential in order to search for the best available subband for all new femtocells when it connects to the core network. When a

femtocell (F_i) is switched on, it registers to the system database. Once the registration is completed, it receives the RSRP values from the MBS and stores them in φ_i^M. On the basis of RSRP values, the system declares approximate location of F_i and its sector. In the next step, the λ sets a group of available subbands and discards the subbands used by macrocell in that sector. Every sector has a group of $\left(K \setminus S\right)$ usable subbands, where K denotes the total number of SBs, S is the number of sectors. Here, '\' indicates exclusion in set theory. Once, the group of available subbands is identified, the algorithm checks all the frequencies received from other femtocells nearby to avoid the co-tier interference. All the RSRP values received at F_i from other femtocells of the same sector are stored in $\varphi_{i,j}^F$, while the RSRP values received from femtocells of other sectors are discarded.

On a ''first come first served'' basis, the first subband from the group of usable subbands λ is assigned to the first active femtocell (F_i) and the second subband to the second active femtocell (F_{i+1}) and so on. Once all the available subbands in the group are assigned to femtocells, in the next step, the RSRP values stored in $\varphi_{i,j}^F$ are checked and the subband having the lowest RSRP value is selected an assigned frequency.

For example, if there are four SBs i.e., B, C, E, and F available for femtocell (F_i) in sector α, by using the proposed algorithm, the first, second, third and fourth deployed femtocells will get subband B, C, E, and F, respectively. Subsequently, when the fifth femtocell turns on in sector α, it searches for available subbands in that particular sector, however it returns with unavailable subband. Afterwards, it checks for the lowest received RSRP values, which are stored in $\varphi_{i,j}^F$. As a result, the farthest subband from this sector wise grouped in λ is assigned to the fifth requesting femtocell. Hence, femtocells have less chances to interfere with each other.

V. PERFORMANCE EVALUATION METRICS

A. SIGNAL TO INTERFERENCE PLUS NOISE RATIO (SINR)

In LTE-A HetNets, the unwanted singals are also received from undesired transmitters in the downlink channel. The downlink SINR value received at UE in LTE-A networks heavily degrades due to the effect of interference that occurs among femtocells and macrocells. For MUE m uses subcarrier k in macrocell M, its SINR is calculated as [29],

$$SINR_m^k = \frac{P_M^k G_{m,M}^k}{N_o \Delta f + \sum_m P_{M'}^k G_{m,M'}^k + \sum_m P_F^k G_{m,F}^k} \quad (5)$$

where P_M^k and $G_{m,M}^k$ denote the transmit power of the macrocell M at subcarrier k and the channel gain of a MUE m from the desired macrocell M at subcarrier k, respectively. N_o is the white noise power density of the subcarrier spacing Δf, which is 15 KHz in LTE-A. $P_{M'}^k$ and $G_{m,M'}^k$ are the transmit power and channel gain at subcarrier k of a MUE m from the interferer macrocells M'. While, the P_F^k and $G_{m,F}^k$ are transmit power and channel gain at subcarrier k of a MUE m from the interferer femtocells F.

Similarly, we obtain the SINR value from femtocell F at subcarrier k of a FUE f, the equation is described as,

$$SINR_f^k = \frac{P_F^k G_{f,F}^k}{N_o \Delta f + \sum_f P_{F'}^k G_{f,F'}^k + \sum_f P_M^k G_{f,M}^k} \quad (6)$$

where P_F^k and $G_{f,F}^k$ indicate the transmit power and the channel gain from the desired femtocell F at subcarrier k of a FUE f, respectively. The $P_{F'}^k$ and $G_{f,F'}^k$ are the transmit power and channel gain at subcarrier k of a FUE f from the undesired femtocell F'. Similarly, the P_M^k and $G_{m,M}^k$ are transmit power and channel gain respectively at subcarrier k of a FUE f from the macrocell M.

B. CHANNEL CAPACITY

The Shannon capacity of the system depends on SINR and system bandwidth, and for macrocell M at subcarrier k, it is calculated as,

$$C_m^k = \Delta f log_2(1 + \alpha SINR_m^k), \quad (7)$$

where, $SINR_m^k$ is the SINR (dB) value of MUE m at subcarrier k, and $\alpha = -1.5/ln(5BER)$. BER denotes the target bit error rate (10^{-6}).

The channel capacity for femtocell (F) is obtained by the following equation,

$$C_f^k = \Delta f log_2(1 + \alpha SINR_f^k), \quad (8)$$

where $SINR_f^k$ is the SINR value of FUE f at subcarrier k.

C. THROUGHPUT

The throughput T_X, $X \in \{M, F\}$ achieved by macrocell M and femtocell F can be written as,

$$T_X = \sum_x \sum_k \psi_x^k C_x^k, \quad X \in \{M, F\}, \; x \in \{m, f\}. \quad (9)$$

where ψ_x^k indicates the subcarrier k assignment to UE x. When $\psi_x^k = 1$, it indicates that the subcarrier k is assigned to UE x, otherwise, $\psi_x^k = 0$.

Total throughput of the system is obtained by summing up the throughputs achieved by femtocells F and macrocells M,

$$T_{total} = T_M + T_F. \quad (10)$$

D. SYSTEM EFFICIENCY

We defined system efficiency (η) is a performance metric as a ratio between number of UEs requested ($N_{UE,r}$) and number of UEs served ($N_{UE,s}$) and is given by,

$$\eta = \frac{N_{UE,s}}{N_{UE,r}} \times 100 \quad (\%). \quad (11)$$

E. USER SATISFACTION

In wireless communication system, the SINR is used to examine the signal quality with respect to interference and noise. The higher SINR value means a better signal quality and UE satisfaction is defined as the probability of obtaining SINR value above or equal the threshold [30],

$$p(\Gamma_{thr}) = p(SINR_{UEs} \geq \Gamma_{thr}) = 1 - F(\Gamma_{thr}) \qquad (12)$$

where F(.) and Γ_{thr} denote Cumulative Distribution Function (CDF) and SINR threshold value.

F. ALGORITHM COMPLEXITY

The asymptotic computational complexity of the proposed FFR-3SL algorithm is analyzed by considering a two-tiered HetNet. We consider that seven macrocells are deployed and there are total of N_{Fc} femtocells in this two-tiered HetNet. The proposed algorithm allocates the most suitable subband to every newly deployed femtocell f_i. In our algorithm, the complexity of the first loop that executes allocation of subbands to each layer (central, middle, and outer layers) in a macrocell and allocates them to sectors is $O(S)$. In order to find the best available subband for every newly deployed femtocell, our algorithm has one outer loop, one inner loop, and a search statement inside the inner loop. Since it uses two loops and one search operation, the complexity of allocating subbands to femtocells is $O(N_{Fc} \times N^s_{Fc} \times N^s_{Fc})$. In the worst case, we assume $N_{Fc} = N^s_{Fc}$, hence complexity will be $O(N^3_{Fc})$. Therefore, the overall computational complexity of the proposed algorithm is $O(S)+O(N^3_{Fc})$, and ignoring the first term, i.e., $S << N^s_{Fc}$, overall complexity becomes $O(N^3_{Fc})$.

TABLE 2. Simulation parameters.

Parameters	*Values*
Carrier Frequency	2.0 GHz
System Bandwidth	20 MHz (LTE-A)
Subcarrier Spacing (Δf)	15 KHz
Total number of RBs (ω)	100
Total number of Macrocells	7
Total number of Femtocells (N_{Fc})	140
No. of Femtocells per Macrocell	20
No. of UEs in one cell	100
Max. no. of UEs per Femtocell	5
Macrocell Radius	500 m
Femtocell Radius	30 m
Macrocell Transmit Powers	[20 , 15 , 10] Watt
Femtocell Transmit Power	20 mWatt
White Noise Power Density	-174 dBm/Hz

VI. SIMULATION MODEL AND RESULTS

Simulations are performed to assess the effectiveness of the proposed method in terms of throughput, capacity and efficiency. Our proposed method, FFR-3SL is also compared with the existing methods, FFR-3, OSFFR, and FFR-3R. Table 2 summarizes the simulation parameters. The two-tiered HetNet is considered with 7 macrocells and total 140 of femtocells. It is assumed that the femtocells are uniformly deployed within a macrocell region. Moreover, each macrocell consists of 100 UEs, which are also uniformly distributed over the macrocell coverage area. Besides, we applied the Round Robin scheduling algorithm and assigned random RBs to users varying from 2 to 10 RBs per UE to satisfy user higher radio resources demand. After setting network parameters, Monte Carlo simulation are performed, by running simulations 100 times. For each simulation run, number of femtocell deployed within macrocell region is increased linearly. The same procedure is executed for other existing FFR methods as well, with the same simulation conditions as in our method.

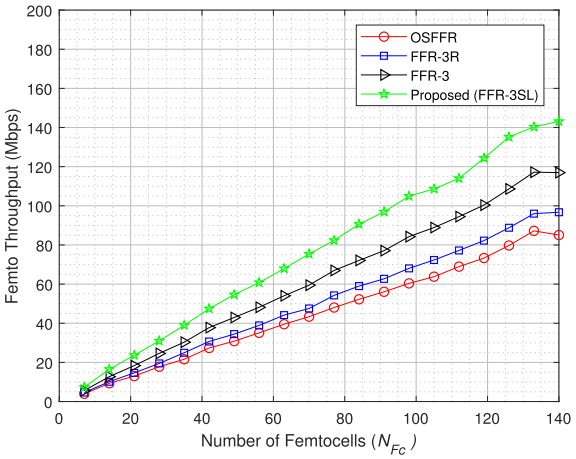

FIGURE 4. Throughput vs number of femtocells (N_{Fc}) for FUEs in two-tier HetNet using FFR algorithms.

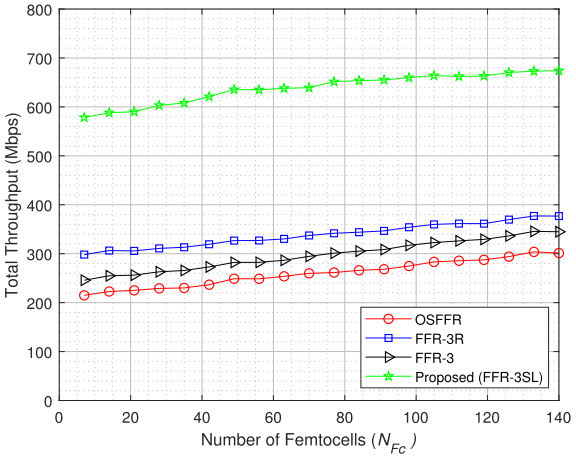

FIGURE 5. Throughput vs number of femtocells (N_{Fc}) for all UEs in two-tier HetNet using FFR algorithms.

Simulation results are presented in Figure 4 through Figure 9. Throughput achieved by FUEs is given in Fig. 4. The proposed FFR-3SL method achieves better throughput as compared to the other three existing methods. For all methods, the throughput increases with the increase in number of femtocells. For instance, when the number of femtocells

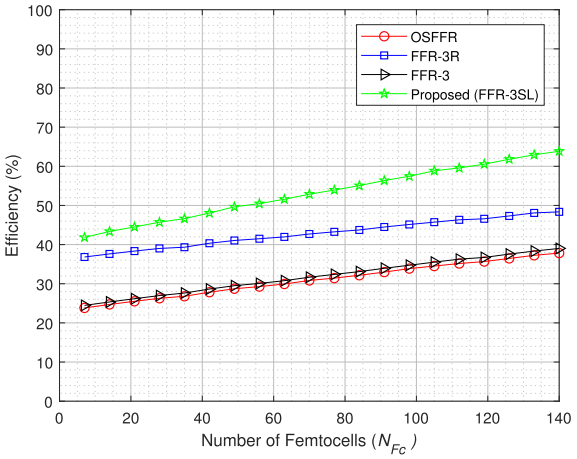

FIGURE 6. System efficiency vs number of femtocells (N_{Fc}) for all UEs in two-tier HetNet using FFR algorithms.

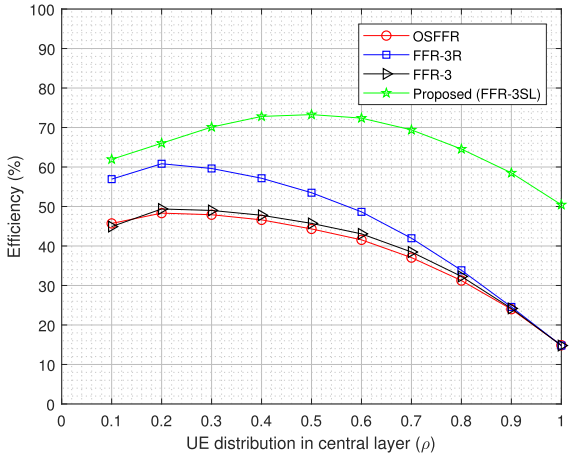

FIGURE 7. The effect of central layer UE distribution on system efficiency using FFR algorithms.

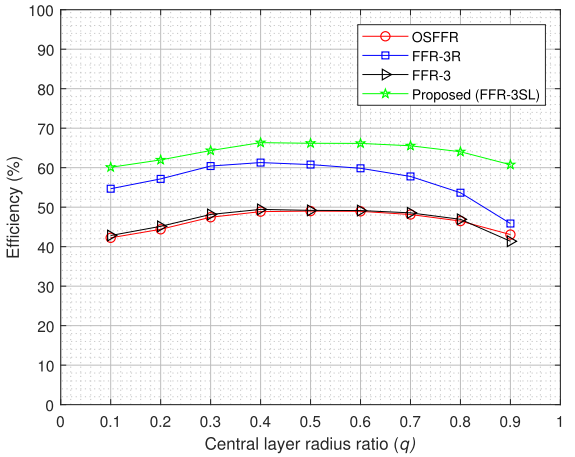

FIGURE 8. The effect of central layer radius on system efficiency using FFR algorithms.

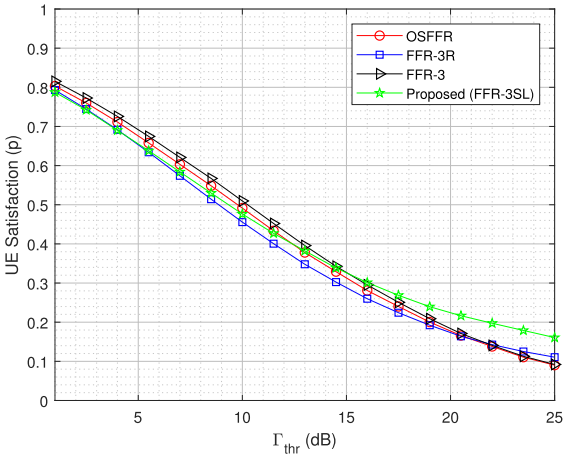

FIGURE 9. The probability of UE satisfaction vs SINR threshold values using FFR algorithms.

reaches up to 100, the proposed FFR-3SL achieves throughput about 105 Mbps, while FFR-3, FFR-3R, and OSFFR methods achieve around 85, 70 and 60 Mbps of throughput, respectively. The performance gap between the proposed method and other existing methods becomes larger as there are more femtocells deployed in the system. When we consider all the UEs in the system, throughput of our proposed method becomes obviously much larger, i.e, more than twice, than that of other methods as shown in the Fig. 5. For instance, when the total number of femtocells is 50, the FFR-3SL achieves above 600 Mbps of throughput while at the same number of femtocells, the FFR-3R method has that is half of the proposed method.

Another performance metric is the efficiency, i.e., UEs connectivity in the system, the results of which are shown in Fig. 6. As the number of femtocells grows, the percentage of UEs connected to the system in the proposed method is higher than that of other methods. As the total number of femtocells reach up to 140, efficiency of the system in the proposed method approaches to almost 65%, while FFR-3R, FFR-3, and OSFFR methods have efficiencies around 49%, 29%, and 28%, respectively.

The user density distribution in central layer is expressed by,

$$\rho = \frac{N_{UE,c}}{N_{UE}}, \quad 0 \leq \rho \leq 1.$$

where $N_{UE,c}$ and N_{UE} denote the number of UEs deployed in central layer and total number of UEs available in macrocell, respectively. Fig. 7 presents the results for evaluation the effect of UE distribution in the central layer on the system efficiency for 140 femtocells. When 50% of UEs is deployed in the central layer, the proposed method achieves the optimum system efficiency, which is nearly 70% of the overall system. On the other hand, the existing methods FFR-3R, FFR-3, and OSFFR achieve largest system efficiencies of about 60%, 50%, and 48%, respectively, for UE distribution ratio (ρ) of 0.2 in the central layer. This indicates that the methods other than the proposed method focus on the outer layers, while the proposed method mainly focuses on the UEs connected in the center zone. The benefit of the center zone

is to give importance to the UEs close to the MBS, which is the main purpose of the HetNet.

In order to investigate the central layer radius on system performance, we define a ratio of central layer radius (r_c) over the whole macrocell radius (R) as,

$$q = \frac{r_c}{R}.$$

Fig. 8 shows the effect of radius of the central layer in a multi-layered HetNet system. All FFR methods achieve optimum efficiency at $q = 0.4$. For instance, at $q = 0.4$, the proposed method achieves the optimum efficiency of about 68%, while the second highest efficiency is achieved by FFR-3R with nearly 62% efficiency. The main idea of using a variable central layer radius is to be able to change it according to the UEs demand and their location.

Fig. 9 provides the results regarding UE satisfaction request to varying SINR threshold (Γ_{thr}) values in dB. The UE satisfaction of the proposed FFR-3SL method surpasses all the other existing methods when ($\Gamma_{thr} = 12$ dB) and above. Fig. 9 also shows that the proposed method satisfies almost half of the UEs having SINR threshold value of 10 dB. All the results in the above figures indicate that the proposed FFR-3SL method achieves not only high throughput but also satisfies the UEs regarding SINR thresholds and center layered zones specification.

VII. CONCLUSION

In this paper, a new FFR scheme is proposed, which maximizes the overall throughput of the LTE-A HetNet by controlling the CCI before it occurs. The total available bandwidth is divided into seven subbands, which are then allocated to macrocells and femtocells in different zones of the macrocell coverage areas. In order to implement our new approach for frequency reuse, we proposed a novel FFR-3SL algorithm, which tries to find the best available subband for a newly deployed femtocell in a macrocell coverage area. Moreover, in order to verify the accuracy of the proposed method a Monte Carlo simulation is implemented. Simulation results confirm that the proposed FFR-3SL method reduces not only the CCI but also improves the throughput and efficiency of the overall system. Furthermore, effect of the UEs resource demand, users density distribution, and variation in the central layer radius on the system performance are investigated and compared with three existing methods. Simulation results show that the proposed approach, FFR-3SL outperforms the other FFR approaches for all considered cases.

REFERENCES

[1] M. Wang, J. Chen, E. Aryafar, and M. Chiang, "A survey of client-controlled hetnets for fifth generation (5G)," *IEEE Access*, vol. 5, pp. 2842–2854, 2017.

[2] P. Cerwall, P. Jonsson, and R. Möller, S. Bävertoft, S. Carson, and I. Godor, "Ericsson mobility report," *On Pulse Networked Society. Hg. v. Ericsson*, 2015.

[3] V. Cisco, "Cisco visual networking index: Forecast and trends, 2017–2022," Cisco, San Jose, CA, USA, White Paper 1, 2018.

[4] Y. Zhou, F. R. Yu, J. Chen, and Y. Kuo, "Resource allocation for information-centric virtualized heterogeneous networks with in-network caching and mobile edge computing," *IEEE Trans. Veh. Technol.*, vol. 66, no. 12, pp. 11339–11351, Dec. 2017.

[5] M. Hasan, A. F. Ismail, A. H. Abdalla, K. Abdullah, H. Ramli, S. Islam, and R. A. Saeed, "Inter-cell interference coordination in LTE-A HetNets: A survey on self organizing approaches," in *Proc. Int. Conf. Comput., Electr. Electron. Eng. (ICCEEE)*, Aug. 2013, pp. 196–201.

[6] K. Mallinson. (2016). *The Path to 5G: As Much Evolution as Revolution*. [Online]. Available: http://www.3gpp.org/news-events/3gpp-news/1774-5g_wiseharbourvisited 01/25/2018

[7] E. Yaacoub, "Green 5G femtocells for supporting indoor generated IoT traffic," in *Internet of Things (IoT) in 5G Mobile Technologies*. New York, NY, USA: Springer, 2016, pp. 129–152.

[8] E. Park, A. del Pobil, and S. Kwon, "The role of Internet of Things (IoT) in smart cities: Technology roadmap-oriented approaches," *Sustainability*, vol. 10, no. 5, p. 1388, May 2018.

[9] Á. Hernández, I. Guío, and A. Valdovinos, "Radio resource allocation for interference management in mobile broadband OFDMA based networks," *Wireless Commun. Mobile Comput.*, vol. 10, no. 11, pp. 1409–1430, Nov. 2010.

[10] S. A. Khan, M. Asshad, K. Kucuk, and A. Kavak, "A power control algorithm (PCA) and software tool for femtocells in LTE-A networks," *Sakarya Univ. J. Sci.*, vol. 22, no. 4, pp. 1124–1129, Aug. 2018.

[11] L. Zhang, L. Yang, and T. Yang, "Cognitive interference management for LTE-A femtocells with distributed carrier selection," in *Proc. IEEE 72nd Veh. Technol. Conf.-Fall*, Sep. 2010, pp. 1–5.

[12] A. Mahmud, Z. Lin, and K. A. Hamdi, "On the energy efficiency of fractional frequency reuse techniques," in *Proc. IEEE Wireless Commun. Netw. Conf. (WCNC)*, Apr. 2014, pp. 2348–2353.

[13] N. A. Ali, M. A. El-Dakroury, M. El-Soudani, H. M. ElSayed, R. M. Daoud, and H. H. Amer, "New hybrid frequency reuse method for packet loss minimization in LTE network," *J. Adv. Res.*, vol. 6, no. 6, pp. 949–955, Nov. 2015.

[14] H.-B. Chang and I. Rubin, "Optimal downlink and uplink fractional frequency reuse in cellular wireless networks," *IEEE Trans. Veh. Technol.*, vol. 65, no. 4, pp. 2295–2308, Apr. 2015.

[15] C. Chen, S. Videv, D. Tsonev, and H. Haas, "Fractional frequency reuse in DCO-OFDM-based optical attocell networks," *J. Lightw. Technol.*, vol. 33, no. 19, pp. 3986–4000, Oct. 1, 2015.

[16] M. T. Kawser, M. R. Islam, K. I. Ahmed, M. R. Karim, and J. B. Saif, "Efficient resource allocation and sectorization for fractional frequency reuse (FFR) in LTE femtocell systems," *Radioengineering*, vol. 24, p. 4, Dec. 2015.

[17] S. Kumar, S. Kalyani, and K. Giridhar, "Impact of sub-band correlation on SFR and comparison of FFR and SFR," *IEEE Trans. Wireless Commun.*, vol. 15, no. 8, pp. 5156–5166, Aug. 2016.

[18] S. Gupta, S. Kumar, R. Zhang, S. Kalyani, K. Giridhar, and L. Hanzo, "Resource allocation for D2D links in the FFR and SFR aided cellular downlink," *IEEE Trans. Commun.*, vol. 64, no. 10, pp. 4434–4448, Oct. 2016.

[19] Y. Li, C. Niu, F. Ye, and R. Q. Hu, "A universal frequency reuse scheme in LTE-A heterogeneous networks," *Wireless Commun. Mobile Comput.*, vol. 16, no. 17, pp. 2839–2851, Dec. 2016.

[20] J. García-Morales, G. Femenias, and F. Riera-Palou, "Statistical analysis and optimization of a fifth-percentile user rate constrained design for FFR/SFR-aided OFDMA-Based cellular networks," *IEEE Trans. Veh. Technol.*, vol. 67, no. 4, pp. 3406–3419, Apr. 2017.

[21] C. Onu, B. Salihu, and J. Abolarinwa, "Enhanced fractional frequency reuse in Lte-A heterogeneous OFDMA network," *ATBU J. Sci., Technol. Edu.*, vol. 6, no. 2, pp. 18–27, May 2018.

[22] N. Saquib, E. Hossain, and D. I. Kim, "Fractional frequency reuse for interference management in LTE-advanced hetnets," *IEEE Wireless Commun.*, vol. 20, no. 2, pp. 113–122, Apr. 2013.

[23] N. Fradi, S. Najeh, and H. Boujemaa, "Resource allocation in OFDMA networks with femto and macro-cells coexistence using fractional frequency reuse (FFR)," in *Proc. 4th Int. Conf. Commun. Netw.*, Mar. 2014, pp. 1–5.

[24] K. Davaslioglu, C. C. Coskun, and E. Ayanoglu, "Energy-efficient resource allocation for fractional frequency reuse in heterogeneous networks," *IEEE Trans. Wireless Commun.*, vol. 14, no. 10, pp. 5484–5497, Oct. 2015.

[25] P. Lee, T. Lee, J. Jeong, and J. Shin, "Interference management in LTE femtocell systems using fractional frequency reuse," in *Proc. 12th Int. Conf. Adv. Commun. Technol. (ICACT)*, vol. 2, Feb. 2010, pp. 1047–1051.
[26] C. S. Park and S. Park, "Analysis of RSRP measurement accuracy," *IEEE Commun. Lett.*, vol. 20, no. 3, pp. 430–433, Mar. 2016.
[27] J. Lee, Y. Kim, Y. Kwak, J. Zhang, A. Papasakellariou, T. Novlan, C. Sun, and Y. Li, "LTE-advanced in 3GPP Rel-13/14: An evolution toward 5G," *IEEE Commun. Mag.*, vol. 54, no. 3, pp. 36–42, Mar. 2016.
[28] S. U. Abdullahi, J. Liu, C. Huang, and X. Zhang, "Enhancing throughput performance in LTE-advanced hetnets with buffered fractional frequency reuse," in *Proc. 8th Int. Conf. Ubiquitous Future Netw. (ICUFN)*, Jul. 2016, pp. 918–923.
[29] M. Çakir and A. Kalaycioglu, "Power adjustment based interference management in dense heterogeneous femtocell networks," in *Proc. 2nd Int. Conf. Comput. Commun. Syst. (ICCCS)*, Jul. 2017, pp. 133–137.
[30] D. B. C. Battikh, "Outage probability formulas for cellular networks: Contributions for MIMO, comp and time reversal features," Ph.D. dissertation, Télécom ParisTech, Paris, France, 2012.

SAJJAD AHMAD KHAN received the B.S. degree in information technology from UET Peshawar and the M.S. degree in telecommunication and computer network from Islamabad, Pakistan. He is currently pursuing the Ph.D. degree with the Department of Computer Engineering, Kocaeli University, Turkey. He is involved in the field of wireless communication. His research interests include radio resource management (RRM) and interference management in LTE-A heterogeneous networks (HetNets).

ADNAN KAVAK received the M.S. and Ph.D. degrees from the Electrical-Computer Engineering Department, The University of Texas at Austin, where he was a Visiting Professor, from 2008 to 2009. He was a Senior Researcher with Samsung Telecommunication America, Dallas, TX, from 2000 to 2001. He is currently a Professor with the Department of Computer Engineering, Kocaeli University, Kocaeli, Turkey. His recent research interests include 5G and beyond wireless communication, cooperative networks, physical layer security in next generation networks, smart antennas and MIMO Systems, synchronization in cloud computing, E-Health systems, and machine learning applications in communication systems.

SULTAN ALDIRMAZ ÇOLAK received the B.S. degree in electronics and communications engineering from Kocaeli University, Kocaeli, Turkey, in 2004, and the M.S. and Ph.D. degrees from Yildiz Technical University (YTU), Istanbul, in 2006 and 2012, respectively. She was a Visiting Research Scholar with the Department of Electrical and Computer Engineering, University of South Florida, in 2009. She is currently an Assistant Professor with the Electronics and Communications Engineering Department, Kocaeli University. Her research interests include time frequency signal processing and communication theory.

KEREM KÜÇÜK received the B.S., M.S., and Ph.D. degrees from the Electronics and Computer Education Department, Kocaeli University, Kocaeli, Turkey, where he is currently an Associate Professor with the Department of Computer Engineering. He was a Guest Researcher and a Visiting Scholar with the Pervasive Systems Group, Twente University, Twente, Netherlands, and the Wireless Information Systems Laboratory, the University of Texas at Dallas, TX, respectively. His research interests include the Internet of Things, vehicular networks, computer and wireless networks, ultrawideband systems, embedded systems, real-time signal processing, and LTE-A systems.